Wind-driven Arctic freshwater anomalies

K. D. Stewart[1] and T. W. N. Haine[1]

Received 7 October 2013; revised 21 November 2013; accepted 21 November 2013; published 11 December 2013.

[1] Large freshwater (FW) anomalies have been observed in the Arctic FW budget and exports in the last decade but their origin is unclear. This letter examines if the large-scale wind conditions might be responsible. We employ an idealized model forced by wind conditions that generate FW budget anomalies. Anticyclonic (cyclonic) winds cause an increase (decrease) of FW in the Western Arctic. For anticyclonic winds, the magnitude and timescale of the FW accumulation in the Western Arctic are similar to observations. Importantly, a cyclonic shift in the winds can only generate a realistically large release event if the Western Arctic is anomalously fresh beforehand. Given that the Western Arctic presently stores excess FW, the findings suggest that a present-day shift to cyclonic winds will generate a large release of liquid FW from the Arctic through the Canadian Arctic Archipelago. **Citation:** Stewart, K. D., and T. W. N. Haine (2013), Wind-driven Arctic freshwater anomalies, *Geophys. Res. Lett.*, *40*, 6196–6201, doi:10.1002/2013GL058247.

1. Introduction

[2] The Arctic Ocean is integral to the northern hemisphere freshwater (FW) loop, facilitating in the catchment and distillation of FW and its subsequent export to the Atlantic [*Carmack and McLaughlin*, 2011]. The annual mean Arctic Ocean liquid freshwater (LFW) budget is $\sim 74,000\,\mathrm{km}^3$ (relative to a salinity of $S = 34.8$), with an additional $10,000$–$15,000\,\mathrm{km}^3$ (for an average thickness of 2–3 m) of FW as sea ice (SI) [*Serreze et al.*, 2006]. This FW inventory is maintained by runoff ($3200\,\mathrm{km}^3/\mathrm{yr}$; [*Serreze et al.*, 2006]), net precipitation less evaporation ($P - E$, $2000\,\mathrm{km}^3/\mathrm{yr}$; [*Serreze et al.*, 2006]), and the residual of ocean inflows from the relatively salty Atlantic and relatively fresh Pacific (the latter contributing $2500\,\mathrm{km}^3/\mathrm{yr}$; [*Woodgate et al.*, 2006]). FW is exported from the Arctic in continental shelf currents through the Canadian Arctic Archipelago (CAA, measured at the Davis Strait at $3600\,\mathrm{km}^3/\mathrm{yr}$; [*Curry et al.*, 2011]) and Fram Strait as liquid ($1960\,\mathrm{km}^3/\mathrm{yr}$; [*de Steur et al.*, 2009]) and SI ($2200\,\mathrm{km}^3/\mathrm{yr}$; [*Kwok*, 2009]). Significant uncertainties exist for these flux estimates, and while the net observed FW flux is indistinguishable from zero ($0(100)\,\mathrm{km}^3/\mathrm{yr}$), the Arctic Ocean has freshened over the last 20 years [*Rabe et al.*, 2013].

[3] Most Arctic FW is contained in the Western Arctic, specifically the Beaufort Gyre, where prevailing anticyclonic winds drive an Ekman convergence of surface FW [*Proshutinsky et al.*, 2002]. By this wind mechanism, the FW content in the Beaufort Gyre increases for anticyclonic and decreases for cyclonic wind conditions, allowing the Beaufort Gyre to accumulate and release FW with rates set by the wind rather than by Arctic FW sources. The present anticyclonic conditions, commencing in the mid-1990s, have led to the large-scale redistribution of FW within the Arctic and an accumulation of FW in the Western Arctic and Beaufort Gyre, recently observed at a rate of $\sim 8000\,\mathrm{km}^3$ in 15 years [e.g., *Proshutinsky et al.*, 2009; *McPhee et al.*, 2009]. It has been suggested that as the summer SI field declines the efficiency of the atmosphere-to-ocean momentum, transfer increases enabling an increased accumulation of FW without a change in the winds [*Giles et al.*, 2012]. The observed accumulation is likely associated with other factors including the increased melting of multiyear SI [e.g., *Yamamoto-Kawai et al.*, 2009; *Korhonen et al.*, 2012], the increase of FW input from Eurasian shelves [*Dmitrenko et al.*, 2008], and the possible increase of Pacific FW inflowing through Bering Strait [*Woodgate et al.*, 2006, 2012].

[4] Previous modeling studies demonstrate that the large-scale winds redistribute FW within the Arctic Ocean [e.g., *Häkkinen and Proshutinsky*, 2004; *Condron et al.*, 2009; *Jahn et al.*, 2010]. They also show that Arctic FW export is influenced by the wind. The impact of the wind on FW export amplitudes, timescales, and pathways is unclear, however. For instance, Arctic FW export variability is thought to have led to the "Great Salinity Anomaly" (GSA) events, which are decadal scale freshenings of the subpolar North Atlantic and Nordic Seas [*Dickson et al.*, 1988; *Belkin et al.*, 1998; *Belkin*, 2004]. These events have been attributed to Arctic FW export anomalies estimated at $10,000\,\mathrm{km}^3$ over 5 years [*Curry and Mauritzen*, 2005] through the Fram Strait as SI [*Dickson et al.*, 1988] or through the CAA as LFW [*Belkin et al.*, 1998; *Belkin*, 2004]; however, the total volume of excess FW associated with a GSA event has never been measured. A link may exist between GSA events and the large-scale wind circulation regime, although it has not yet been formalized [e.g., *Dickson et al.*, 2000]. Previous work indicates that changes in wind conditions lead to FW export anomalies reaching only half the magnitude estimated for a GSA scale event [*Condron et al.*, 2009].

[5] The fate of Arctic FW anomalies is uncertain. It is hypothesized that a cyclonic change in wind conditions will lead to a release of FW from the Beaufort Gyre and the Arctic with implications for North Atlantic Deep Water (NADW) formation [e.g., *Jahn et al.*, 2010]. To influence NADW formation, the extra FW must affect the source waters of NADW, namely the dense water overflowing the Greenland-Scotland Ridge or the water present in the deep convection zones of the Labrador and Irminger Seas. FW anomalies leave the Arctic in narrow, intense surface

[1]Department of Earth and Planetary Sciences, Johns Hopkins University, Baltimore, Maryland, USA.

Corresponding author: K. D. Stewart, Department of Earth and Planetary Sciences, Johns Hopkins University, Olin Hall, 3400 North Charles St., Baltimore, 21218 MD, USA. (kialstewart@jhu.edu)

0094-8276/13/10.1002/2013GL058247

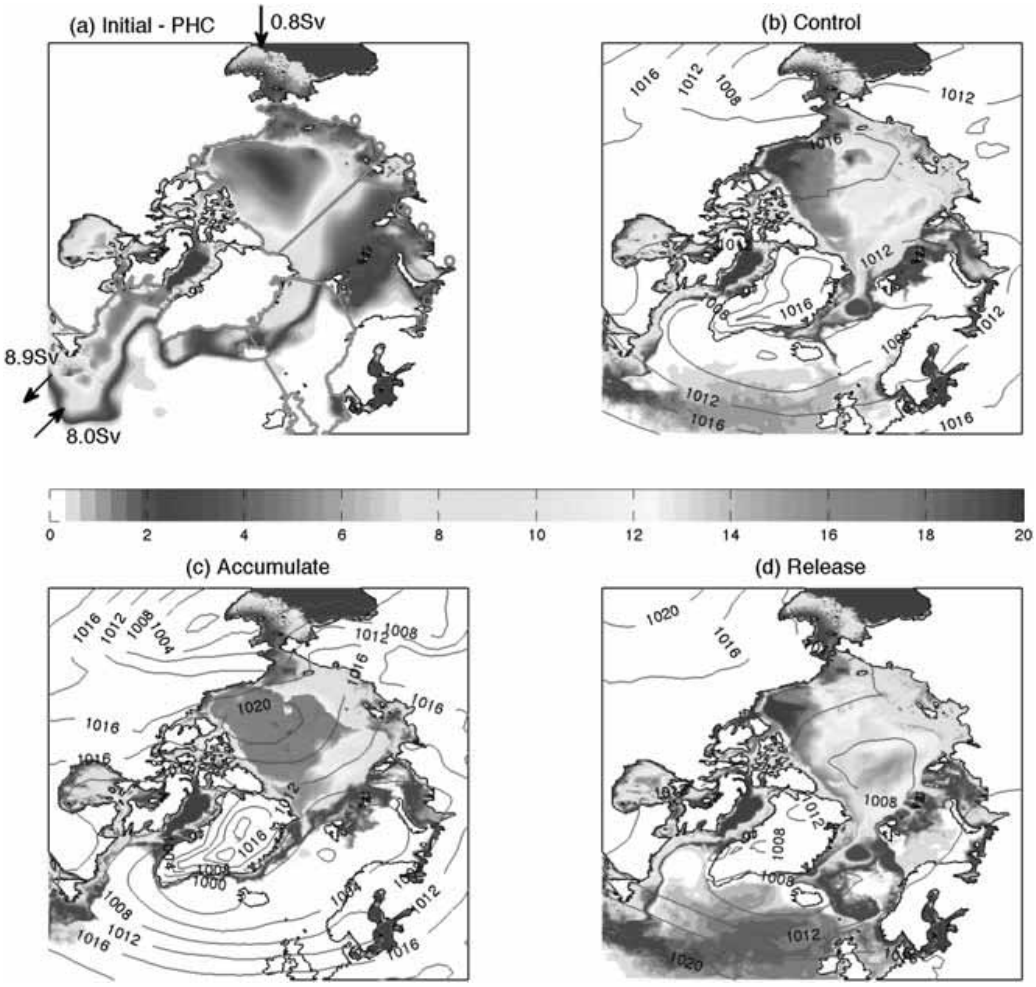

Figure 1. Liquid freshwater (m) distributions for (a) the initial condition (developed from the PHC data set), and the annual means of the (b) *Control*, (c) *Accumulate* and (d) *Release* runs at 20 years. The approximate locations of the river mouths (red circles) and prescribed oceanic fluxes (arrows) are shown in Figure 1a, with the Western Arctic, Atlantic, and Nordic regions used for Figure 2 outlined in magenta. The sea level pressure fields (hPa) for the three different wind forcings are overlain in Figures 1b–1d.

currents on the shelves, however, and do not immediately access the NADW source waters. The processes controlling the transfer of FW anomalies from the shelf currents to the NADW source waters are poorly understood. For example, the transfer processes in circulation models depend on the representation of shelf currents and in particular on shelf-basin exchange. Models with horizontal grid spacing around 100 km exhibit broad diffuse shelf currents with rapid shelf-basin exchange, thus exaggerating the sensitivity of NADW formation to Arctic FW export anomalies [e.g., *Jahn et al.*, 2010]. Models with grid spacing of a few tens of kilometers represent the shelf break and shelf currents, but fail to resolve shelf-basin exchange adequately which can trap FW anomalies on the shelves and away from NADW source waters [e.g., *Myers*, 2005]. At about 10 km resolution, shelf-basin exchange is better resolved and FW export anomalies can be transported from the shelves by eddies to NADW source waters [e.g., *McGeehan and Maslowski*, 2011]. Accurately capturing shelf-basin exchange involving dense cascades requires higher resolution; a 2 km grid seems to suffice [*Magaldi et al.*, 2011].

[6] Here we ask, can the wind generate Arctic FW budget and FW export anomalies of the magnitudes and timescales of those observed? Specifically, can changes in the wind cause (a) the Western Arctic FW inventory to increase 8000 km^3 in 15 years and (b) the Arctic to release 10,000 km^3 in 5 years? We build upon previous studies investigating the relationship between the wind and the FW budget [e.g., *Condron et al.*, 2009; *Jahn et al.*, 2010], by employing an idealized circulation model of the Arctic Ocean forced with wind conditions favorable for generating FW budget anomalies.

2. Model and Methodology

[7] We use the coupled ice-ocean components of the MITgcm [*Marshall et al.*, 1997] in hydrostatic mode to simulate the circulation in the Arctic and North Atlantic regions (Figure 1a). A $\frac{1}{8}^\circ$ ($\sim$ 13 km) rotated coordinate curvilinear grid is employed with 50 vertical levels ranging in resolution from 5 m at the surface to 300 m at the maximum depth of 5500 m; 25 levels occupy the upper 350 m.

Bathymetry is interpolated from the ETOPO1 global relief model [*Amante and Eakins*, 2009]. Initial hydrographic conditions come from the Polar Science Center Hydrographic Climatology 3.0 database (PHC, [*Steele et al.*, 2001]). The Pan-Arctic Ice-Ocean Modeling and Assimilation System data set (PIOMAS, [*Zhang and Rothrock*, 2003]) is used to develop the initial SI field.

[8] Steady oceanic volume fluxes are imposed into the domain at the Pacific (0.8 Sv; 1 Sv = 10^6 m^3/s) and Atlantic (8.0 Sv) boundaries, with locations and hydrographic properties representative of the Bering Strait Inflow and North Atlantic Current, respectively. Steady runoff from the 13 largest Arctic rivers, totaling 0.1 Sv (3200 km^3/yr of LFW), is prescribed as per the Arctic Ocean Model Intercomparison Project (www.whoi.edu/page.do?pid=30587). These inflows are balanced by outflows totaling 8.9 Sv prescribed at the Atlantic boundary to represent the Labrador Current and southward flowing North Atlantic Intermediate and Deep Waters.

[9] The wind forcing is the only input parameter varied. The control wind field (CON) is the 1948–2011 mean of the NCEP/NCAR record. Anomaly wind fields are taken from the 2007 winter and 1989 summer mean wind fields; these periods have been identified as most favorable for accumulating (ACC) and releasing (REL) freshwater to/from the Beaufort Gyre, respectively [*Proshutinsky et al.*, 2011]. The corresponding sea level pressure fields for the CON, ACC, and REL wind fields are shown in Figures 1b–1d. The atmospheric temperature and radiative fluxes are held constant at the 1948–2011 mean of the NCEP/NCAR reanalysis product [*Kalnay et al.*, 1996], and evaporation and precipitation (including snow) are set to zero.

[10] The model is run from rest for 60 years with CON wind forcing to develop a *Control* state, which is used to initialize three separate single forcing runs: one continues with the CON winds, one with the ACC winds, and one with the REL winds (*Control*, *Accumulate*, and *Release* runs, respectively). After 20 years with *Accumulate* (*Release*) winds, the Western Arctic reaches a state of FW excess (deficit), and the wind forcing is switched to the alternate anomaly wind condition, giving two composite forcing runs (*Acc-Rel*, and *Rel-Acc*). This suite allows direct comparison of both (a) the response of the FW budget to changes in wind conditions, and (b) the sensitivity of this response to the ocean's state (i.e., FW excess or deficit).

[11] We focus on the FW inventories of the Western Arctic, North Atlantic, and Nordic Seas (outlined in magenta, Figure 1a) and the FW exports through the major Arctic gateways (Lancaster, Nares, Davis, and Fram Straits, Figure 3). Liquid freshwater is quantified by $\mathrm{LFW}(x,y,t) = \int_{D(x,y,t)}^{0}(1 - S(x,y,t)/S_{\mathrm{ref}})\,\mathrm{d}z$,, where S_{ref} (= 34.8) is a reference salinity, D is the depth of the S_{ref} isohaline surface, and z is the vertical coordinate. LFW, S, and D vary in space (x,y) and time t. Sea ice density, thickness, and concentration are used to calculate the solid freshwater contribution, which is added to the LFW to give the total freshwater (TFW) content.

[12] For simplicity we omit $P - E$, the smallest of the three major LFW contributors to the Arctic. Excluding $P - E$ removes complications associated with the sea ice model (such as sublimation and snow-dependent albedo) that would otherwise require parameter tuning and/or flux adjustment to avoid model drift. Omitting $P - E$ means that the LFW export fluxes are likely to be systematically lower than the observed fluxes.

[13] For simplicity we also omit the seasonal cycle. Seasonality is important for sea ice whose inventory doubles because of winter freezing. This seasonal SI either leaves through Fram Strait, melts, or survives the subsequent summer to become multiyear SI. This seasonal SI is also the main cause of seasonal variability of the Arctic LFW inventory, estimated to be ±8% [*Serreze et al.*, 2006]: seasonal variability of the TFW inventory is much lower. Removing seasonality eliminates seasonal SI and produces a model SI field that is thicker, older, and less mobile, although the volume is close to the observed annual average. For these reasons we expect the model SI export through Fram Strait to be biased low. Although such persistent forcing conditions are physically unrealistic, the simulations grant insight into FW anomaly generation and adjustment processes.

3. Results and Discussion

3.1. Spin-Up

[14] Following an initial ∼40 year adjustment period, the model approaches a quasi-steady state without significant drift in the temperature, salinity or FW fields. The FW distribution arising from the CON winds reproduces the large-scale features of the PHC data set (Figure 1a,b), such as the Western Arctic and CAA FW intensification and fresh tongue extending through Fram Strait. We do not expect the idealized forcing of the CON winds to exactly reproduce the hydrographic record (developed from observations spanning decades). Nevertheless, the success of the simplified model in this respect illustrates the robustness of the dynamics governing the Arctic FW distribution. The TFW inventory of the Western Arctic is steady at 62, 000 km^3, within 5% of the initial condition (65, 000 km^3, Figure 2a). The FW fluxes through the major Arctic gateways are steady and similar to the observations (Figure 3). They are in general less than the observed fluxes, however, especially in the Fram Strait. This is expected as the model omits LFW input from P–E, a major contributor to the Fram Strait LFW export. SI export through Fram Strait is also less than the observed annual average, which we attribute to the absence of a seasonal cycle.

3.2. Single Forcing Runs

[15] The initial response of the FW distribution to a change in winds is consistent with previous modeling studies [e.g., *Häkkinen and Proshutinsky*, 2004; *Condron et al.*, 2009]; within 15 years, the Western Arctic is in a state of FW excess or deficit. For ACC (REL) winds, the Western Arctic FW inventory increases 18% to 73, 000 km^3 (decreases 5% to 58, 000 km^3), with the opposite occurring in the subpolar Atlantic and Nordic regions (Figure 2). For the *Accumulate* run, this increase (∼ 10, 000 km^3 over 20 years) compares well with the recent observed increase of 8000 km^3 over 15 years [e.g., *McPhee et al.*, 2009]. However, for the *Release* run, the switch to REL winds from the *Control* state leads to a decrease in Western Arctic TFW (∼ 5000 km^3 over 15 years) and subsequent increase in Atlantic TFW that is too small and too slow compared to a GSA-scale event (estimated to be ∼ 10, 000 km^3 over 5 years).

[16] The FW export flux responses are more complicated. Shifting to ACC winds has a rapid (0(1) year) and

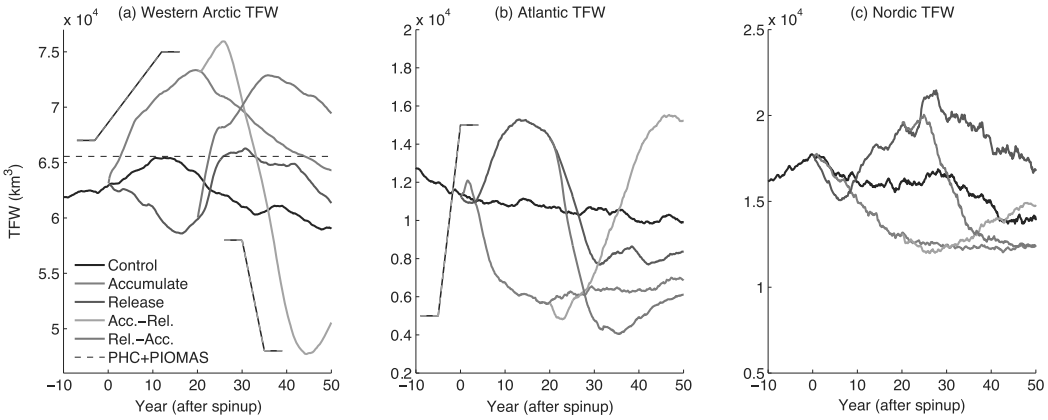

Figure 2. Time series of the (a) Western Arctic, (b) Atlantic, and (c) Nordic TFW content (these regions are shown in Figure 1a). The red-black and green-black lines reflect changes of 8000 km^3 over 15 years and 10,000 km^3 over 5 years, respectively. Note the different scales.

sustained impact, with the LFW export through the CAA decreasing to approximately half that of the *Control* run. SI export through the Fram Strait significantly increases because the Transpolar Drift (TPD) strengthens (see isobars of Figure 1c) accelerating central Arctic SI export through the Fram Strait. This increased SI export for ACC winds is reminiscent of the GSA paradox described by *Dickson et al.* [2000]; the increased Fram Strait SI export responsible for the 1970s GSA occurred when the large-scale winds favored FW accumulation in the Western Arctic. In this case, the increased FW export through Fram Strait derives from regions other than the Western Arctic; specifically, thick SI from the shelves north of Greenland and the CAA and the Eurasian Basin is directed through Fram Strait by a strengthened TPD. Shifting to REL wind forcing is less dramatic. An initial pulse of increased LFW export through the CAA and decreased LFW export through Fram Strait lasts for approximately a decade, after which the fluxes return to *Control* values. There is a negligible Fram Strait SI export response. Interestingly, the changes in FW export fluxes east and west of Greenland largely compensate, such that a shift to either of the anomaly wind forcings from the *Control* state generates a muted response in the net Arctic FW export. This highlights the primary influence of the wind regimes: the large-scale redistribution of FW within the Arctic.

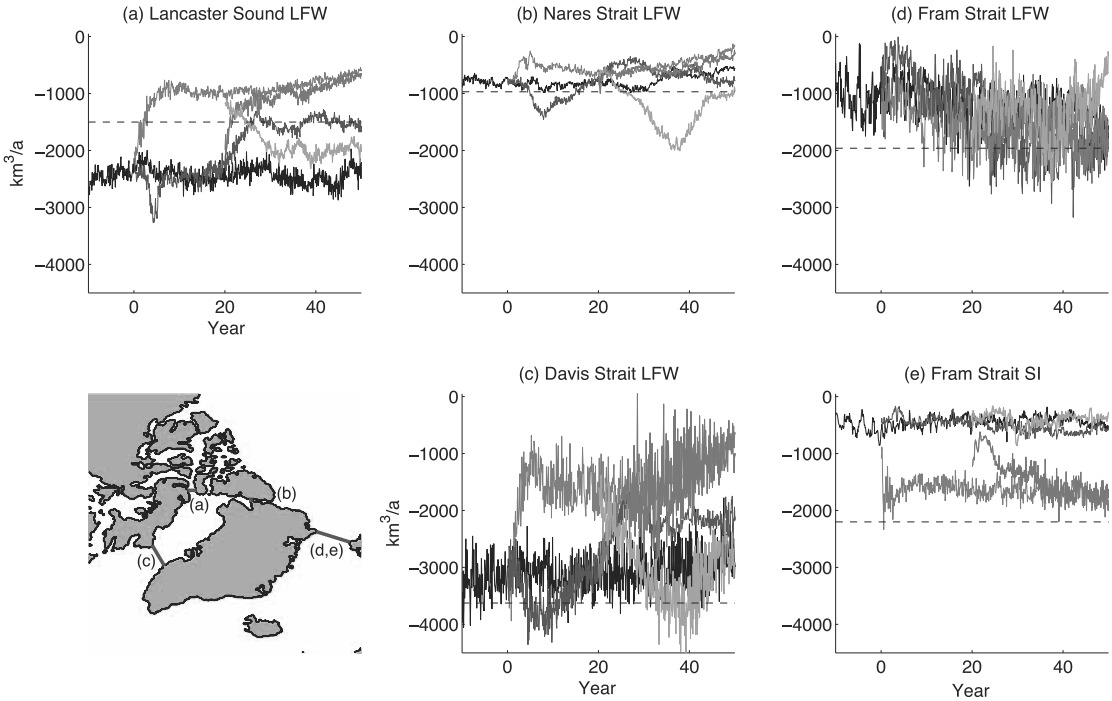

Figure 3. FW exports through the main Arctic gateways. The observations are from (a) *Prinsenberg and Hamilton* [2005], (b) *Münchow et al.* [2007], (c) *Curry et al.* [2011], (d) *de Steur et al.* [2009], and (e) *Kwok* [2009]. Line coloring is the same as Figure 2.

[17] After ∼20 years of sustained anomaly winds, the FW inventory of the Western Arctic begins to return toward *Control* levels, reflecting a recirculation of the FW anomaly throughout the domain. Following the initial shift from CON winds, the FW anomaly (negative or positive) is first detected in the Western Arctic, then subsequently in the CAA and Baffin Bay, Labrador Shelf, subpolar Atlantic, Nordic Seas, Eastern Arctic, and Siberian Shelves and ultimately returns to the Western Arctic where it brings the FW inventory back toward the *Control* state. The FW anomaly propagates as an incoherent and basin scale signal. The propagation and recirculation timescales are perhaps model dependent and may be influenced by domain size and atmospheric feedbacks, among other omitted processes. Nevertheless, they are broadly consistent with GSA spreading [*Belkin et al.*, 1998; *Belkin*, 2004]. Even for the most favorable wind conditions, the generation and dispersal of wind-driven Arctic FW anomalies occur over decades.

3.3. Composite Forcing Runs

[18] A significantly greater Arctic FW export anomaly is generated for a cyclonic shift in the winds when the Western Arctic is in a state of FW excess, as seen in the *Acc-Rel* run. For this case the Western Arctic FW inventory decreases at a rate similar to that estimated for GSA events ($29,000\,\mathrm{km}^3$ over 20 years; Figure 2a). The net Arctic FW export flux anomaly (relative to the *Control* run) of the *Acc-Rel* run peaks at $\sim 1,700\,\mathrm{km}^3/\mathrm{yr}$. The pathway for this increased FW release is entirely through the CAA and is best detected in the Nares Strait which has the greatest signal-to-noise ratio (Figure 3b). The amplitude, timescale, and pathway of this significant FW release is qualitatively similar to those responsible for the 1980s and 1990s GSA events [*Belkin et al.*, 1998; *Belkin*, 2004]. Auxiliary runs (not shown) demonstrate that the extreme cyclonic conditions of the REL winds are not necessary to elicit a large FW export event: any cyclonic shift in the winds at a time of FW excess in the Western Arctic results in significant FW export. Unlike the FW excess state, the response of the FW deficit state to a change in wind is not significantly different to that of the *Control* state (see *Rel–Acc* run in Figures 2 and 3). The results of the composite forcing runs indicate that the Arctic FW budget is particularly sensitive to a cyclonic shift in the wind when the Western Arctic is in a state of FW excess. This preconditioning couples with the close proximity of the LFW inventory anomaly to the CAA gateways to provide a trigger mechanism for the rapid release of LFW from the Arctic.

3.4. Impact on NADW Formation

[19] The model shows that exported Arctic FW resides preferentially in shelf currents (Figures 1b–1d). The mean salinity of the upper 300 m on the Greenland and Labrador Shelves varies by around $\Delta S = 1$ for ACC and REL winds (relative to the *Control* run). In regions of deep convection (Labrador and Nordic basins), the change is at most $\Delta S = 0.1$ and lags the change in shelf salinities by almost a decade. Using a model with 9 km horizontal resolution, *McGeehan and Maslowski* [2011] find changes in shelf salinities of a similar magnitude to those seen here. They find that upper ocean salinity in the Labrador Sea deep convection region varies by as much as the shelf currents, however, and on a faster timescale than seen here; in these cases the fresh anomalies are large enough to halt deep convection. This result suggests that the present model sufficiently resolves the shelf currents but underestimates the Labrador shelf-basin exchange (perhaps because there is no wind-forced variability). Shelf-basin exchange is also known to occur on even smaller scales. For example, *Magaldi et al.* [2011] use a 2 km resolution model to study cascading off the East Greenland shelf which influences the Denmark Strait Overflow and hence NADW. For this reason, it is unclear what resolution is required to accurately model shelf-basin exchange and the impact of Arctic FW export anomalies on NADW formation, perhaps as short as 0(1) km. Nevertheless, the present findings show that changes in the large-scale Arctic wind freshen the subpolar shelves sufficiently to impact NADW if a mechanism exists to transport them intact to the NADW formation regions.

4. Conclusions

[20] An idealized model has been used to examine the extent to which changing wind conditions influence the Arctic FW budget. The model exhibits a response to the wind consistent with previous studies; for anticyclonic (cyclonic) winds, there is an increase (decrease) of FW in the Western Arctic. The FW inventories of the major Arctic and subpolar basins respond to changes in the winds on a decadal timescale; FW export fluxes respond on a more rapid 0(1) yr timescale. Anticyclonic winds drive FW accumulation in the Western Arctic of a magnitude and timescale similar to recent observations. Shifting to a cyclonic wind regime at a time of FW excess in the Western Arctic generates a GSA scale FW release through the CAA. The associated freshening of the current on the Labrador continental shelf is likely sufficient to impact NADW formation by deep convection in the Labrador basin if the shelf-basin exchange does not significantly dilute the anomaly. Considering that the Western Arctic is currently in a state of FW excess, we expect significant FW release through the CAA if the present-day winds shift toward a cyclonic regime.

[21] **Acknowledgments.** We thank I. Belkin and two anonymous referees for their helpful comments to improve this manuscript. We are supported by the National Science Foundation grant 0904338. Numerical simulations were conducted using the Homewood High Performance Compute Cluster of the Johns Hopkins University. Special thanks to C. Hill for assistance configuring the model and to A. Fuller, S. Jeffress, and I. Koszalka for insightful discussion and comments.

[22] The Editor thanks Igor Belkin and two anonymous reviewers for their assistance in evaluating this paper.

References

Amante, C., and B. W. Eakins (2009), ETOPO1 1 arc-minute global relief model: Procedures, data sources and analysis, *NOAA Tech. Memo.*, *NESDIS NGDC-24*, National Geophysical Data Center, Boulder, Colo.

Belkin, I. M., S. Levitus, J. Antonov, and S.-A. Malmberg (1998), "Great Salinity Anomalies" in the North Atlantic, *Prog. Oceanogr.*, *41*, 1–68.

Belkin, I. M. (2004), Propagation of the "Great Salinity Anomaly" of the 1990s around the northern North Atlantic, *Geophys. Res. Lett.*, *31*, L08306, doi:10.1029/2003GL019334.

Carmack, E., and F. McLaughlin (2011), Towards recognition of physical and geochemical change in Subarctic and Arctic Seas, *Prog. Oceanogr.*, *90*, 90–104.

Condron, A., P. Winsor, C. Hill, and D. Menemenlis (2009), Simulated response of the Arctic freshwater budget to extreme NAO wind forcing, *J. Clim.*, *22*, 2422–2437.

Curry, R., and C. Mauritzen (2005), Dilution of the northern North Atlantic Ocean in recent decades, *Science*, *308*, 1772–1774.

Curry, B., C. M. Lee, and B. Petrie (2011), Volume, freshwater, and heat fluxes through Davis Strait, 2004–05, *J. Phys. Oceanogr.*, *41*, 429–436.

de Steur, L., E. Hansen, R. Gerdes, M. Karcher, E. Fahrbach, and J. Holfort (2009), Freshwater fluxes in the East Greenland Current: A decade of observations, *Geophys. Res. Lett.*, *36*, L23611, doi:10.1029/2009GL041278.

Dickson, R. R., J. Meincke, S.-A. Malmberg, and A. Lee (1988), The "Great Salinity Anomaly" in the Northern North Atlantic 1968–1982, *Prog. Oceanogr.*, *20*, 103–151.

Dickson, R. R., T. J. Osborn, J. W. Hurrell, J. Meincke, J. Blindheim, B. Adlandsvik, T. Vinje, G. Alekseev, and W. Maslowski (2000), The Arctic Ocean response to the North Atlantic oscillation, *J. Clim.*, *13*, 2671–2696.

Dmitrenko, I. A., S. A. Kirillov, and L. B. Tremblay (2008), The long-term and interannual variability of summer fresh water storage over the eastern Siberian shelf: Implication for climatic change, *J. Geophys. Res.*, *113*, C03007, doi:10.1029/2007JC004304.

Giles, K. A., S. W. Laxon, A. L. Ridout, D. J. Wingham, and S. Bacon (2012), Western Arctic Ocean freshwater storage increased by wind-driven spin-up of the Beaufort Gyre, *Nat. Geosci.*, *5*, 194–197.

Häkkinen, S., and A. Proshutinsky (2004), Freshwater content variability in the Arctic Ocean, *J. Geophys. Res.*, *109*, C03051, doi:10.1029/2003JC001940.

Jahn, A., B. Tremblay, L. A. Mysak, and R. Newton (2010), Effect of the large-scale atmospheric circulation on the variability of the Arctic Ocean freshwater export, *Clim. Dyn.*, *34*, 201–222.

Kalnay, E., et al. (1996), The NCEP/NCAR 40-year reanalysis project, *Bull. Am. Meteorol. Soc.*, *77*, 437–471.

Korhonen, M., B. Rudels, M. Marnela, A. Wisotzki, and J. Zhao (2012), Time and space variability of freshwater content, heat content and seasonal ice melt in the Arctic Ocean from 1991 to 2011, *Ocean Sci. Discuss.*, *9*, 2621–2677.

Kwok, R. (2009), Outflow of Arctic Ocean sea ice into the Greenland and Barents Seas: 1979–2007, *J. Clim.*, *22*, 2438–2457.

Magaldi, M. G., T. W. N. Haine, and R. S. Pickart (2011), On the nature and variability of the East Greenland spill jet: A case study in summer 2003, *J. Phys. Oceanogr.*, *41*, 2307–2327.

Marshall, J., A. Adcroft, C. Hill, L. Perelman, and C. Heisey (1997), A finite-volume, incompressible Navier Stokes model for studies of the ocean on parallel computers, *J. Geophys. Res.*, *102*, 5753–5766.

McGeehan, T., and W. Maslowski (2011), Impact of shelf-basin freshwater transport on deep convection in the Western Labrador sea, *J. Phys. Oceanogr.*, *41*, 2187–2210.

McPhee, M. G., A. Proshutinsky, J. H. Morison, M. Steele, and M. B. Alkire (2009), Rapid change in freshwater content of the Arctic Ocean, *Geophys. Res. Lett.*, *36*, L10602, doi:10.1029/2009GL037525.

Münchow, A., K. K. Falkner, and H. Melling (2007), Spatial continuity of measured seawater and tracer fluxes through Nares Strait, a dynamically wide channel bordering the Canadian Archipelago, *J. Mar. Res.*, *65*, 759–788.

Myers, P. G. (2005), Impact of freshwater from the Canadian Arctic Archipelago on Labrador Sea Water formation, *Geophys. Res. Lett.*, *32*, L06605, doi:10.1029/2004GL022082.

Prinsenberg, S. J., and J. Hamilton (2005), Monitoring the volume, freshwater and heat fluxes passing through Lancaster Sound in the Canadian Arctic Archipelago, *Atmos. Ocean*, *43*(1), 1–22.

Proshutinsky, A., R. H. Bourke, and F. A. McLaughlin (2002), The role of the Beaufort Gyre in Arctic climate variability: Seasonal to decadal climate scales, *Geophys. Res. Lett.*, *29*(23), 2100, doi:10.1029/2002GL015847.

Proshutinsky, A., R. Krishfield, M.-L. Timmermans, J. Toole, E. Carmack, F. McLaughlin, W. J. Williams, S. Zimmermann, M. Itoh, and K. Shimada (2009), Beaufort Gyre freshwater reservoir: State and variability from observations, *J. Geophys. Res.*, *114*, C00A10, doi:10.1029/2008JC005104.

Proshutinsky, A., et al. (2011), Recent advances in Arctic ocean studies employing models from the Arctic Ocean Model Intercomparison Project, *Oceanography*, *24*(3), 102–113.

Rabe, B., M. Karcher, F. Kauker, U. Schauer, J. M. Toole, R. A. Krishfield, S. Pisarev, T. Kikuchi, and J. Su (2013), Arctic Ocean liquid freshwater storage trend 1992–2012, *Geophys. Res. Lett.*, in press.

Serreze, M. C., A. P. Barrett, A. G. Slater, R. A. Woodgate, K. Aagaard, R. B. Lammers, M. Steele, R. Moritz, M. Meredith, and C. M. Lee (2006), The large-scale freshwater cycle of the Arctic, *J. Geophys. Res.*, *111*, C11010, doi:10.1029/2005JC003424.

Steele, M., R. Morley, and W. Ermold (2001), PHC: A global ocean hydrography with a high-quality Arctic Ocean, *J. Clim.*, *14*, 2079–2087.

Woodgate, R. A., K. Aagaard, and T. J. Weingartner (2006), Interannual changes in the Bering Strait fluxes of volume, heat and freshwater between 1991 and 2004, *Geophys. Res. Lett.*, *33*, L15609, doi:10.1029/2006GL026931.

Woodgate, R. A., T. J. Weingartner, and R. Lindsay (2012), Observed increases in Bering Strait oceanic fluxes from the Pacific to the Arctic from 2001 to 2011 and their impacts on the Arctic Ocean water column, *Geophys. Res. Lett.*, *39*, L24603, doi:10.1029/2012GL054092.

Yamamoto-Kawai, M., F. A. McLaughlin, E. C. Carmack, S. Nishino, K. Shimada, and N. Kurita (2009), Surface freshening of the Canada Basin, 2003–2007: River runoff versus sea ice meltwater, *J. Geophys. Res.*, *114*, C00A05, doi:10.1029/2008JC005000.

Zhang, R., and D. A. Rothrock (2003), Modeling global sea ice with a thickness and enthalpy distribution model in generalized curvilinear coordinates, *Mon. Weather Rev.*, *131*, 845–861.